GAVIN PUBLISHERS

Archives of Natural and Medicinal Chemistry

Branton A, et al. Arch Nat Med Chem: ANMC-118.

Research Article

DOI: 10.29011/ANMC-118. 000018

The Effect of Consciousness Energy Healing Treatment on Physico-chemical and Thermal Properties of 6-Mercaptopurine

Alice Branton[1], Mahendra Kumar Trivedi[1], Dahryn Trivedi[1], Gopal Nayak[1], Snehasis Jana[2*]

[1]Trivedi Global, Inc., Henderson, USA

[2]Trivedi Science Research Laboratory Pvt. Ltd., India

[*]**Corresponding author:** Snehasis Jana, Trivedi Science Research Laboratory Pvt. Ltd., India. Tel: +9102225811234; Email: publication@trivedisrl.com

Citation: Branton A, Trivedi MK, Trivedi D, Nayak G, Jana S (2018) The Effect of Consciousness Energy Healing Treatment on Physicochemical and Thermal Properties of 6-Mercaptopurine. Arch Nat Med Chem: ANMC-118. DOI: 10.29011/ANMC-118. 000018

Received Date: 21 August, 2018; **Accepted Date:** 17 September, 2018; **Published Date:** 25 September, 2018

Abstract

6-Mercaptopurine is an antimetabolite antineoplastic agent. The objective of the study was to evaluate the impact of the Trivedi Effect®-Consciousness Energy Healing Treatment on physicochemical and thermal properties of 6-mercaptopurine using the modern analytical technique. The 6-mercaptopurine sample was divided into two parts, one part of mercaptopurine was considered as a control sample, while the other part was subjected to the Biofield Treatment remotely by a renowned Biofield Energy Healer, Alice Branton and termed as a treated sample. The PXRD peak intensities and crystallite sizes were significantly altered ranging from -63.38% to 3.85% and -55.26% to 228.26%, respectively, whereas the average crystallite size was significantly increased by 8.16% in the treated mercaptopurine compared with the control sample. The particle size values were significantly decreased by 26.63% (d_{10}), 24.43% (d_{50}), 17.56% (d_{90}), and 21.41% [D (4,3)] and the specific surface area was significantly increased by 38.57% in the treated sample compared to the control sample. The latent heat of fusion was significantly increased by 49.97% in the treated sample compared to the control sample. The total weight loss was decreased by 11.45%; whereas the residue amount was significantly increased by 160.07% in the treated sample compared with the control sample. The results indicated that the Trivedi Effect® might lead to the generation of a new polymorphic form of mercaptopurine which would offer better solubility, absorption, and bioavailability compared with the control sample, which would be useful in designing novel pharmaceutical formulations for the better therapeutic responses against leukemia, Crohn's disease, ulcerative colitis, etc.

Keywords: Consciousness Energy Healing Treatment; DSC; Particle Size; Surface Area; TGA/DTG PXRD; The Trivedi Effect®; 6-Mercaptopurine

Introduction

6-mercaptopurine is an antimetabolite antineoplastic agent. It has immunosuppressant properties. The mechanism of action involves interference with nucleic acid synthesis by inhibiting purine metabolism [1,2]. It is used as a medication for cancer and autoimmune diseases, i.e., acute lymphocytic leukaemia, chronic myeloid leukaemia, Crohn's disease, and ulcerative colitis [3-5]. It was approved for medical use in the United States since 1953 and also listed as Essential Medicines by the World Health Organization [6]. Common side effects associated with the mercaptopurine therapy are diarrhoea, nausea, vomiting, loss of appetite, mouth sores, stomach and abdominal pain, fatigue, weakness, fever, sore throat, skin rash, pinpoint red spots on the skin, darkening of the skin, yellowing of eyes or skin, hair loss, easy bruising or bleeding, dark urine, black or tarry stools, bloody stools, bloody urine, painful or difficult urination, may suppress the production of blood cells (both white and red blood cells) and can be linked to the genetic polymorphisms [7-9]. Mercaptopurine is used in the pharmaceutical formulations for oral medications in the form of tablets and in liquid suspension [10-12]. Mercaptopurine is insoluble in water, acetone, chloroform, and diethyl ether, but slightly soluble in dilute sulphuric acid; and soluble in hot alcohol and dilute alkali solutions [12]. Many scientific communities throughout the globe are researching ways to improve solubility, dissolution, absorption, and bioavailability of pharmaceutical and nutraceutical compounds because the physicochemical properties

of pharmaceutical or nutraceutical compounds are very important [13].

The Trivedi Effect®-Biofield Energy Healing Treatment has shown a significant impact in the alterations of physicochemical properties such as crystallite size, particle size, surface area, thermal behaviour, and bioavailability profile of pharmaceutical and nutraceutical compounds [14-18]. Every living organism possesses a unique para-dimensional electromagnetic field around the body which generated from the continuous movement of the electrically charged particles (ions, cells, etc.), blood flow, and heart moments inside the body known as "Biofield" (Putative Energy Field). The Trivedi Effect® (Biofield Energy) is a natural and is the only scientifically proven phenomenon in which a person can harness this inherently intelligent energy from the Universe and transmit it anywhere on the planet through the possible mediation of neutrinos [19]. Due to the increasing beneficial effects of Complementary and Alternative Medicine (CAM) therapies and integrative healthcare approaches including the Biofield Energy Therapies, alternative medicine is an emerging field treatment methods against various health conditions [20,21]. CAM therapies has been recognized by National Center of Complementary and Integrative Health (NCCIH) along with other therapies, which include Ayurvedic medicine, naturopathy, homeopathy, Tai Chi, Qi Gong, acupuncture, acupressure, healing touch, Reiki, hypnotherapy, Rolfing, etc. The CAM has been accepted by the most of the U.S. population because of several advantages [22,23].

Similarly, the Trivedi Effect®-Consciousness Energy Healing Treatment has significant impact on the transformation in non-living materials and living organisms, and the outcomes were published in numerous peer-reviewed scientific journals. The Trivedi Effect®-Biofield Energy Treatment has the unprecedented capability to transform the physicochemical, structural, and behavioural properties of organic compounds [24,25], metals [26,27], ceramics [28], polymers [29], microorganisms [30,31], living cells [32,33], to improve the overall productivity of crops [34,35], and alter several qualities of metals and ceramics [36,37]. Alice Branton (the USA) is a renowned Biofield Energy Healer. She has the ability to harness Life Force from nature and transmit it to living and non-living object(s), anywhere in the world through thought intention, to change their characteristics, transform their behaviour and enhance their function. She is on a mission to winner the breakthrough science of Life Force Energy and its applications in pharmaceutical and nutraceuticals product research to usher in a new era of human health and wellness. The current study was carried out to evaluate the impact of the Trivedi Effect®-Consciousness Energy Healing Treatment by Alice Branton on the physicochemical, thermal, and behavioural properties of 6-mercaptopurine using powder x-ray diffraction (PXRD), particle size analysis (PSA), differential scanning calorimetry (DSC), and thermogravimetric analysis (TGA)/ differential thermogravimetric analysis (DTG).

Materials and Methods

Chemicals and Reagents

6-Mercaptopurine monohydrate was purchased from Tokyo Chemical Industry Co., Ltd., Japan. All other chemicals used during the experiments were of analytical grade available in India.

Consciousness Energy Healing Treatment Strategies

6-mercaptopurine was the test sample for the experiment, which divided into two equal parts. One part of mercaptopurine was treated with The Trivedi Effect®-Energy of Consciousness Healing Treatment remotely under standard laboratory conditions for 3 minutes and known as The Trivedi Effect® Treated (or Biofield Energy Treated) sample. This Biofield Energy Treatment was provided through the healer's unique energy transmission process by the renowned Biofield Energy Healer, Alice Branton, USA, to the mercaptopurine. However, the second part of mercaptopurine was considered as a control sample (to this no Biofield Energy Treatment was provided). Further, the control sample was treated with a "sham" healer for the comparison purposes. The "sham" healer did not have any knowledge about the Biofield Energy Treatment. After treatment, the Biofield Energy Treated and untreated samples were kept in sealed conditions and characterized using PXRD, PSA, DSC, and TGA techniques.

Characterization

Powder X-ray Diffraction (PXRD) Analysis

The PXRD analysis of mercaptopurine was performed with the help of Rigaku MiniFlex-II Desktop X-ray diffractometer (Japan) [38,39]. The Cu Kα radiation source tube output voltage used was 30 kV, and tube output current was 15 mA. Scans were performed at room temperature. The average size of individual crystallites was calculated from PXRD data using the Scherrer's formula (1):

$$G = k\lambda/\beta\cos\theta \qquad (1)$$

Where k is the equipment constant (0.94), G is the crystallite size in nm, λ is the radiation wavelength (0.154056 nm for Kα1 emission), β is the full-width at half maximum (FWHM), and θ is the Bragg angle [40].

The percent change in crystallite size (G) of mercaptopurine was calculated using the following equation 2:

$$\%\ \text{change in crystallite size} = \frac{[G_{Treated} - G_{Control}]}{G_{Control}} \times 100 \qquad (2)$$

Where $G_{Control}$ and $G_{Treated}$ are the crystallite size of the control and the Biofield Energy Treated samples, respectively.

Particle Size Analysis (PSA)

The particle size analysis of mercaptopurine was conducted on Malvern Mastersizer 2000, (UK) with a detection range between 0.01 µm to 3000 µm using wet method [41,42]. The sample unit (Hydro MV) was filled with a dispersant medium (sunflower oil) and operated the stirrer at 2500 rpm. The PSA analysis of mercaptopurine was performed to obtain the average particle size distribution. Where d (0.1) µm, d (0.5) µm, d (0.9) µm represent particle diameter corresponding to 10% 50% and 90% of the cumulative distribution. D(4,3) represents the average mass-volume diameter, and SSA is the specific surface area (m^2/g). The calculations were done by using software Mastersizer Ver. 5.54.

The percent change in particle size (d) for mercaptopurine at below 10% level (d_{10}), 50% level (d_{50}), 90% level (d_{90}), and D (4,3) was calculated using the following equation 3:

$$\%\ \text{change in particle size} = \frac{[d_{Treated} - d_{Control}]}{d_{Control}} \times 100 \quad (3)$$

Where $d_{Control}$ and $d_{Treated}$ are the particle size (µm) for at below 10% level (d_{10}), 50% level (d_{50}), and 90% level (d_{90}) of the control and the Biofield Energy Treated samples, respectively.

The percent change in surface area (S) was calculated using the following equation 4:

$$\%\ \text{change in surface area} = \frac{[S_{Treated} - S_{Control}]}{S_{Control}} \times 100 \quad (4)$$

Where $S_{Control}$ and $S_{Treated}$ are the surface area of the control and the Biofield Energy Treated mercaptopurine, respectively.

Differential Scanning Calorimetry (DSC)

The DSC analysis of mercaptopurine was performed with the help of DSC Q200, TA instruments. The sample of ~1-2 mg was loaded to the aluminium sample pan at a heating rate of 10ºC/ min from 30°C to 350°C [41,42]. The % change in melting point (T) was calculated using the following equation 5:

$$\%\ \text{change in melting point} = \frac{[T_{Treated} - T_{Control}]}{T_{Control}} \times 100 \quad (5)$$

Where $T_{Control}$ and $T_{Treated}$ are the melting point of the control and treated samples, respectively.

The percent change in the latent heat of fusion (ΔH) was calculated using the following equation 6:

$$\%\ \text{change in latent heat of fusion} = \frac{[\Delta H_{Treated} - \Delta H_{Control}]}{\Delta H_{Control}} \times 100 \quad (6)$$

Where $\Delta H_{Control}$ and $\Delta H_{Treated}$ are the latent heat of fusion of the control and treated mercaptopurine, respectively.

Thermal Gravimetric Analysis (TGA) / Differential Thermogravimetric Analysis (DTG)

TGA/DTG thermograms of mercaptopurine were obtained with the help of TGA Q50 TA instruments. The sample of ~2-5 mg was loaded to the platinum crucible at a heating rate of 10°C/ min from 25°C to 1000°C with the recent literature [41,42]. The % change in weight loss (W) was calculated using the following equation 7:

$$\%\ \text{change in weight loss} = \frac{[W_{Treated} - W_{Control}]}{W_{Control}} \times 100 \quad (7)$$

Where $W_{Control}$ and $W_{Treated}$ are the weight loss of the control and the Biofield Energy Treated mercaptopurine, respectively.

The % change in maximum thermal degradation temperature (T_{max}) (M) was calculated using the following equation 8:

$$\%\ \text{change in Tmax (M)} = \frac{[M_{Treated} - M_{Control}]}{M_{Control}} \times 100 \quad (8)$$

Where $M_{Control}$ and $M_{Treated}$ are the T_{max} values of the control and the Biofield Energy Treated mercaptopurine, respectively.

Results and Discussion

Powder X-ray Diffraction (PXRD) Analysis

The PXRD diffractograms of the control and the Biofield Energy Treated sample showed sharp and intense peaks (Figure 1). These sharp and intense peaks in the chromatograms indicated that both the samples were crystalline. The PXRD diffractograms of the control and the Biofield Energy Treated mercaptopurine samples showed the highest peak intensity at 2θ near to 27.47° and 27.36° (Table 1, entry 10). The peak intensities of the Biofield Energy Treated mercaptopurine were significantly altered compared to the control sample. Overall, the peak intensities of the Biofield Energy Treated sample were significantly altered in the range from -63.38% to 3.85% compared to the control sample (Table 1). Likewise, the crystallite sizes of the Biofield Energy Treated sample were significantly altered in the range from -55.26% to 228.26% compared to the control sample (Table 1). Overall, the average crystallite size of the Biofield Energy Treated mercaptopurine (320.65 nm) was significantly increased by 8.16% compared with the control sample (296.45 nm) (Table 1).

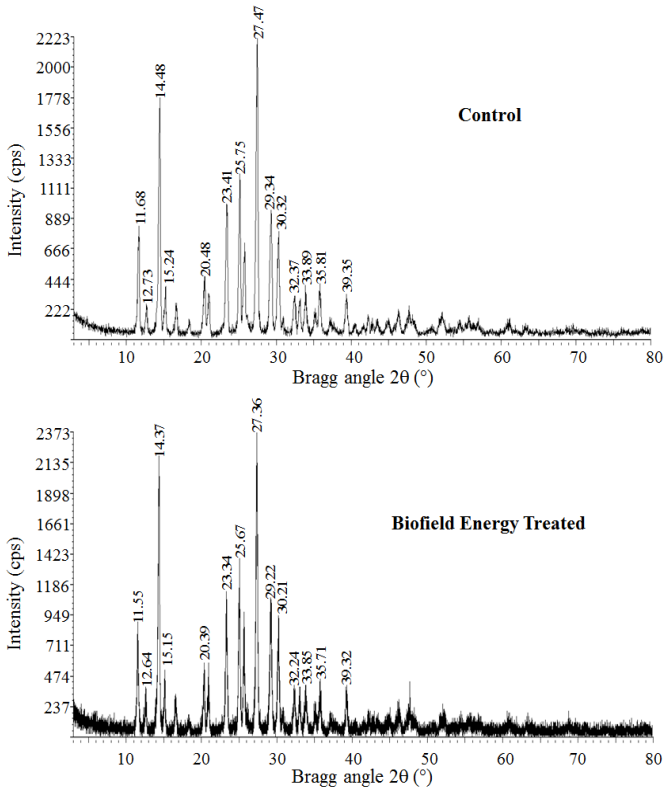

Figure 1: PXRD diffractograms of the control and the Biofield Energy Treated mercaptopurine.

Entry No.	Bragg angle (°2θ)		Peak Intensity (%)			Crystallite size (G, nm)		
	Control	Treated	Control	Treated	% change [a]	Control	Treated	% change [b]
1	11.68	11.55	140	128	-8.57	311	321	3.22
2	12.73	12.64	39	34	-12.82	789	353	-55.26
3	14.48	14.37	364	378	3.85	297	347	16.84
4	15.24	15.15	59	52	-11.86	319	400	25.39
5	16.69	16.6	45	37	-17.78	298	341	14.43
6	20.48	20.39	87	84	-3.45	261	303	16.09
7	21.04	20.94	61	62	1.64	269	313	16.36

8	23.41	23.34	209	181	-13.40	289	345	19.38
9	25.75	25.67	139	140	0.72	287	372	29.62
10	27.47	27.36	457	395	-13.57	291	313	7.56
11	29.34	29.22	208	198	-4.81	268	274	2.24
12	30.32	30.21	160	141	-11.88	280	308	10.00
13	32.37	32.24	57	58	1.75	292	478	63.70
14	33.89	33.85	62	60	-3.23	268	316	17.91
15	35.81	35.71	91	57	-37.36	263	283	7.60
16	39.35	39.32	60	47	-21.67	267	413	54.68
17	42.24	42.22	22	13	-40.91	489	453	-7.36
18	46.39	46.29	35	30	-14.29	244	220	-9.84
19	48.06	47.66	72	62	-13.89	101	109	7.92
20	56.74	55.57	71	26	-63.38	46	151	228.26
21	Average crystallite size					296.45	320.65	8.16

[a]denotes the percentage change in the peak intensity of the Biofield Energy Treated sample with respect to the control sample;
[b]denotes the percentage change in the crystallite size of the Biofield Energy Treated sample with respect to the control sample.

Table 1: PXRD data for the control and the Bio field Energy Treated mercaptopurine.

The peak intensity of each diffraction face on the crystalline compound changes according to the crystal morphology [43] and alterations in the PXRD pattern provide the proof of polymorphic transitions [44,45]. Therefore, any change observed in the crystallite sizes and peak intensities indicated the modification of the crystal morphology of the Biofield Energy Treated mercaptopurine compared to the control sample. The Trivedi Effect®-Consciousness Energy Healing Treatment probably produced a new polymorphic form of mercaptopurine through the Biofield Energy *via* neutrino oscillations [19]. Different polymorphic forms of pharmaceuticals have the significant effects on the drug performance, such as bioavailability, therapeutic efficacy, and toxicity, because of their thermodynamic and physicochemical properties like melting point, energy, stability, and especially solubility, are different from the original form [46,47]. Thus, it can be assumed that the Trivedi Effect® Treated mercaptopurine would be more efficacious in pharmaceutical formulations.

Particle Size Analysis (PSA)

The particle size distribution analysis of both the samples was performed to analyse the change in the particle size, and surface area of the Biofield Energy Treated mercaptopurine compared to the control sample, and the data are presented in (Table 2). The particle size values of the control mercaptopurine at d_{10}, d_{50}, d_{90}, and D (4,3) were 34.82 µm, 99.13 µm, 190.68 µm, and 107.03 µm, respectively. Similarly, the particle sizes of the Biofield Energy

Treated mercaptopurine at d_{10}, d_{50}, d_{90}, and D (4,3) were 25.55 µm, 74.91 µm, 157.20 µm, and 84.11 µm, respectively. The particle size values in the Biofield Energy Treated mercaptopurine were significantly decreased at d_{10}, d_{50}, d_{90}, and D (4,3) by 26.63%, 24.43%, 17.56%, and 21.41% compared to the control sample. Therefore, the specific surface area of the Biofield Energy Treated mercaptopurine (0.134 m^2/g) was significantly increased by 38.57% compared to the control sample (0.0967 m^2/g). Hence, it can be assumed that the Trivedi Effect®-Consciousness Energy Healing Treatment might act as an external force for the conversion of the larger particles into smaller particles, thus increasing the surface area. It was reported that the particle size, shape, and surface area impact the solubility, dissolution rate, absorption, bioavailability, and even the therapeutic efficacy of a drug [47,48]. The solubility of mercaptopurine is almost insoluble in water, acetone, chloroform, and diethyl ether, whereas slightly soluble in dilute sulphuric acid; soluble in hot alcohol and dilute alkali solutions [12]. Thus, it is anticipated that the Biofield Energy Treated mercaptopurine would show the better therapeutic properties in pharmaceutical formulations by increasing solubility, dissolution, and absorption, which would be better for the pharmaceutical industry when used as a raw material for manufacturing.

Parameter	d_{10} (µm)	d_{50} (µm)	d_{90} (µm)	D(4,3) (µm)	SSA (m^2/g)
Control	34.82	99.13	190.68	107.03	0.0967
Biofield Treated	25.55	74.91	157.20	84.11	0.134
Percent change* (%)	-26.63	-24.43	-17.56	-21.41	38.57

d_{10}, d_{50}, and d_{90}: particle diameter corresponding to 10%, 50% and 90% of the cumulative distribution, D (4,3): the average mass-volume diameter, and SSA: the specific surface area.

*denotes the percentage change in the Particle size distribution of the Biofield Energy Treated sample with respect to the control sample.

Table 2: Particle size distribution of the control and the Biofield Energy Treated mercaptopurine.

Differential Scanning Calorimetry (DSC) Analysis

DSC thermograms of both control and the Biofield Energy Treated mercaptopurine are presented in (Figure 2). The DSC thermograms of the control and the Biofield Energy Treated mercaptopurine showed two sharp endothermic peaks in the thermograms (Figure 2). The 1st peak indicated the peak of evaporation of the bounded water from 6-mercaptopurine monohydrate. Similarly, the 2nd peak indicated the melting point of 6-mercaptopurine. The thermogram pattern and melting point closely matched to the literature reported data [49]. The evaporation and melting point of the Biofield Energy Treated mercaptopurine were slightly altered by 0.49% and -0.44%, respectively compared with the control sample (Table 3).

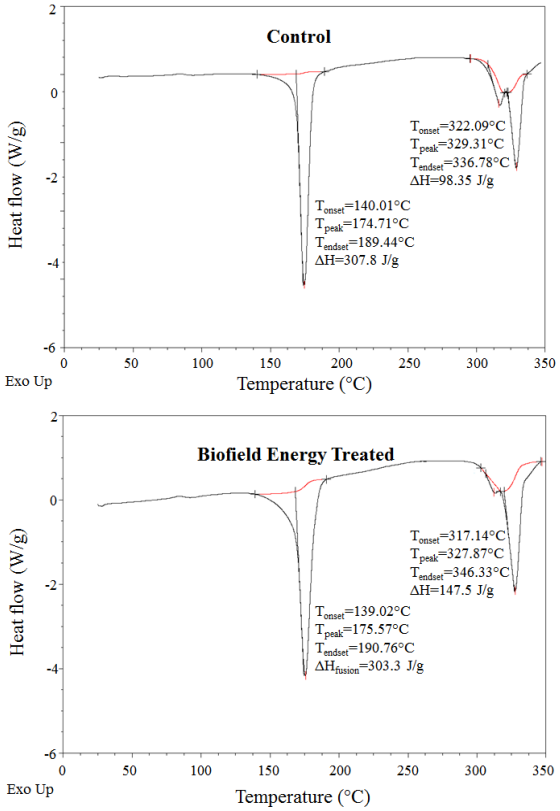

Figure 2: DSC thermograms of the control and the Biofield Energy Treated mercaptopurine.

Sample	Evaporation Temp (˚C)	Melting Point (˚C)	ΔH (J/g)	
			Evaporation	Fusion
Control Sample	174.71	329.31	307.8	98.35
Biofield Energy Treated	175.57	327.87	303.3	147.50
% Change*	0.49	-0.44	-1.46	49.97
ΔH: Latent heat of evaporation/decomposition; *denotes the percentage change of the Biofield Energy Treated mercaptopurine with respect to the control sample.				

Table 3: DSC data for both control and the Bio field Energy Treated samples of mercaptopurine.

The latent heat of evaporation ($\Delta E_{vaporation}$) of the Bio Field Energy Treated mercaptopurine (303.3 J/g) was slightly decreased by 1.46% compared with the control sample (307.8 J/g) (Table 3). However, the latent heat of fusion (ΔH_{fusion}) of the Bio Field Energy Treated mercaptopurine (147.5 J/g) was significantly increased by 49.97% compared with the control sample (98.35 J/g) (Table 3). As per the literature, any change in the latent heat of fusion can be attributed to the disrupted molecular chains and the crystal structure [50]. Thus, it can be predicted that the Trivedi Effect®-Consciousness Energy Healing Treatment might be responsible for the disruption of the molecular chains and crystal structure of mercaptopurine. The evaporation and melting temperatures of the Biofield Energy Treated samples did not alter much compared to the control sample, but the significant increase in the latent heat of fusion indicated that the thermal stability of the Biofield Energy Treated sample was increased compared to the control sample.

Thermal Gravimetric Analysis (TGA)/Differential Thermogravimetric Analysis (DTG)

The TGA thermograms of the control and the Biofield Energy Treated mercaptopurine samples showed three steps of thermal degradation (Figure 3). The total weight loss of the Biofield

Energy Treated mercaptopurine was decreased by 11.45% compared to the control sample (Table 4). Therefore, the residue amount was significantly increased by 160.07% in the Biofield Energy Treated mercaptopurine compared to the control sample (Table 4).

Sample	TGA		DTG; T_{max} (°C)		
	Total weight loss (%)	Residue %	1st Peak	2nd Peak	3rd Peak
Control	93.33	6.68	164.45	335.8	676.1
Biofield Energy Treated	82.64	17.36	160.73	334.3	678.3
% Change*	-11.45	160.07	-2.26	-0.46	0.33
*denotes the percentage change of the Biofield Energy Treated sample with respect to the control sample; T_{max} = the temperature at which maximum weight loss takes place in TG or peak temperature in DTG;					

Table 4: TGA/DTG data of the control and the Biofield Energy Treated samples of mercaptopurine.

The DTG of the control and the Biofield Energy Treated mercaptopurine also showed three peaks in the thermograms (Figure 4). The maximum thermal degradation temperature (T_{max}) of the 1st, 2nd and 3rd peaks of the Biofield Energy Treated sample altered by -2.26%, -0.46%, and 0.33% compared with the control sample (Table 4). Overall, TGA/DTG analysis of mercaptopurine samples revealed that the thermal stability of the Biofield Energy Treated sample was increased compared with the control sample. The improved thermal stability would improve the quality and self-life of mercaptopurine in the pharmaceutical formulations.

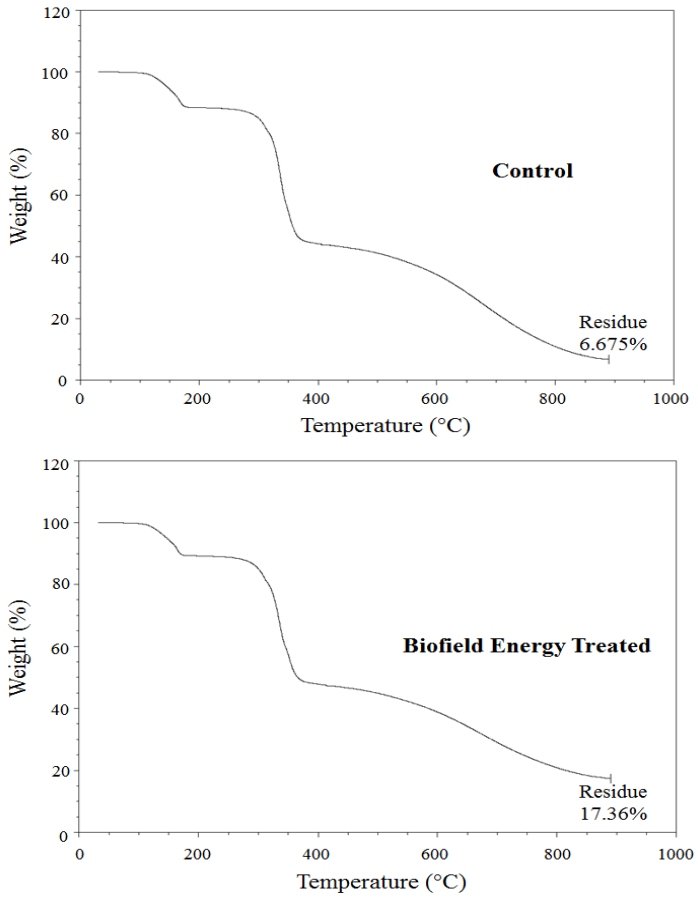

Figure 3: TGA thermograms of the control and the Biofield Energy Treated mercaptopurine.

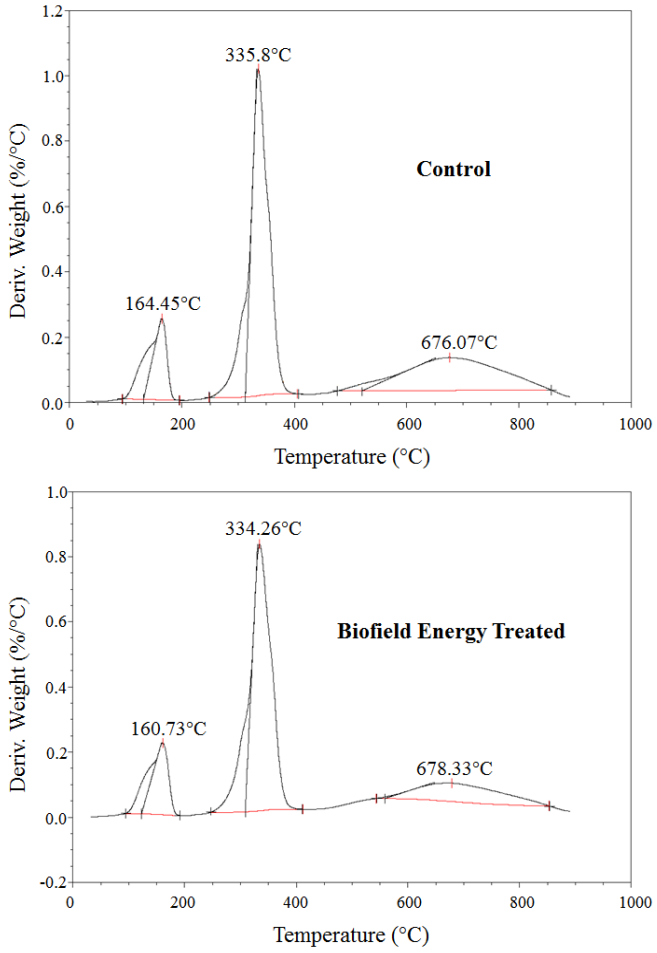

Figure 4: DTG thermograms of the control and the Biofield Energy Treated mercaptopurine.

Conclusion

The experimental results confirmed that the Trivedi Effect®-Consciousness Energy Healing Treatment has significant effects on the particle size, surface area, and thermal properties of 6-mercaptopurine. The PXRD analysis indicated that the peak intensities and crystallite sizes of the Biofield Energy Treated mercaptopurine were significantly altered in the range from -63.38% to 3.85% and -55.26% to 228.26%, respectively compared to the control sample. The average crystallite size of the Biofield Energy Treated mercaptopurine was significantly increased by 8.16% compared with the control sample. The particle size values in the Biofield Energy Treated mercaptopurine were significantly decreased by 26.63%, 24.43%, 17.56%, and 21.41% at d_{10}, d_{50}, d_{90}, and D (4,3) compared to the control sample. Therefore, the specific surface area of the Biofield Energy Treated mercaptopurine was significantly increased by 38.57% compared to the control sample. The significant increase in the ΔH_{fusion} by 49.97% in the Biofield Energy Treated mercaptopurine indicated that the thermal stability of the Biofield Energy Treated sample was more compared to the control sample. The total weight loss was decreased by 11.45%; however, the residue amount was significantly increased by 160.07% in the Biofield Energy Treated sample compared with the control sample. The Trivedi Effect®-Consciousness Energy Healing Treatment might lead to the generation of a new polymorphic form of mercaptopurine which would offer better solubility, dissolution, absorption, and bioavailability compared with the control sample. The Trivedi Effect®-Consciousness Energy Healing Treated mercaptopurine would be more efficacious in pharmaceutical formulations that might offer better therapeutic response against acute lymphocytic leukemia, chronic myeloid leukemia, Crohn's disease, and ulcerative colitis, etc.

Acknowledgements

The authors are grateful to Central Leather Research Institute, SIPRA Lab. Ltd., Trivedi Science, Trivedi Global, Inc., Trivedi Testimonials, and Trivedi Master Wellness for their assistance and support during this work.

Conflict of Interest

Authors declare no conflict of interest.

References

1. Salser JS, Balis ME (1965) The mechanism of action of 6-mercaptopurine: I. biochemical effects. Cancer Res 25: 539-543.
2. https://www.drugbank.ca/drugs/DB01033. Retrieved on 12 February 2018.
3. Present DH, Korelitz BI, Wisch N, Glass JL, Sachar DB, et al. (1980) Treatment of Crohn's disease with 6-mercaptopurine: A long-term, randomized, double-blind study. N Engl J Med 302: 981-798.
4. Schmiegelow K, Glomstein A, Kristinsson J, Björk O (1997) Impact of morning versus evening schedule for oral methotrexate and 6-mercaptopurine on relapse risk for children with acute lymphoblastic leukemia. Nordic Society for Pediatric Hematology and Oncology (NOPHO). J Pediatr Hematol Oncol 19:102-109.
5. Sack DM, Peppercorn MA (1983) Drug therapy of inflammatory bowel disease. Pharmacotherapy 3: 158-176.
6. World Health Organization. WHO Model List of Essential Medicines (April 2015).
7. https://en.wikipedia.org/wiki/Mercaptopurine. Retrieved on 14 February 2018.
8. Yang JJ, Landier W, Yang W, Liu C, Hageman L, et al. (2015) Inherited NUDT15 variant is a genetic determinant of mercaptopurine intolerance in children with acute lymphoblastic leukemia. J Clin Oncol 33: 1235-1242.
9. Moriyama T, Nishii R, Perez-Andreu V, Yang W, Klussmann FA, et al. (2016) NUDT15 polymorphisms alter thiopurine metabolism and hematopoietic toxicity. Nature Genet 48: 367-373.

10. Lerner EI, Flashner-Barak M, Achthoven EV, Keegstra H, Smit R (2012) Formulations of 6-mercaptopurine. US patent US8188067 B2.

11. Tiphaine Ade B, Hjalgrim LL, Nersting J, Breitkreutz J, Nelken B, et al. (2016) Evaluation of a pediatric liquid formulation to improve 6-mercaptopurine therapy in children. Eur J Pharm Sci 83: 1-7.

12. (2018) https://pubchem.ncbi.nlm.nih.gov/compound/6-Mercaptopurine.

13. Chereson R (2009) Bioavailability, bioequivalence, and drug selection. In: Makoid CM, Vuchetich PJ, Banakar UV (Eds) Basic pharmacokinetics (1st Edn) Pharmaceutical Press, London.

14. Trivedi MK, Patil S, Shettigar H, Bairwa K, Jana S (2015) Effect of biofield treatment on spectral properties of paracetamol and piroxicam. Chem Sci J 6: 98-104.

15. Trivedi MK, Patil S, Shettigar H, Bairwa K, Jana S (2015) Spectroscopic characterization of biofield treated metronidazole and tinidazole. Med chem 5: 340-344.

16. Branton A, Jana S (2017) The influence of energy of consciousness healing treatment on low bioavailable resveratrol in male Sprague Dawley rats. International Journal of Clinical and Developmental Anatomy 3: 9-15.

17. Branton A, Jana S (2017) The use of novel and unique biofield energy healing treatment for the improvement of poorly bioavailable compound, berberine in male Sprague Dawley rats. American Journal of Clinical and Experimental Medicine 5: 138-144.

18. Branton A, Jana S (2017) Effect of the biofield energy healing treatment on the pharmacokinetics of 25-hydroxyvitamin D_3. [25(OH)D_3] in rats after a single oral dose of vitamin D3. American Journal of Pharmacology and Phytotherapy 2: 11-18.

19. Trivedi MK, Mohan TRR (2016) Biofield energy signals, energy transmission and neutrinos. American Journal of Modern Physics 5: 172-176.

20. Barnes PM, Bloom B, Nahin RL (2008) Complementary and alternative medicine use among adults and children: United States, 2007. Natl Health Stat Report 12: 1-23.

21. Frass M, Strassl RP, Friehs H, Müllner M, Kundi M, et al. (2012) Use and acceptance of complementary and alternative medicine among the general population and medical personnel: A Systematic Review. Ochsner J 12: 45-56.

22. Koithan M (2009) Introducing complementary and alternative therapies. J Nurse Pract 5: 18-20.

23. Rubik B (2002) The biofield hypothesis: Its biophysical basis and role in medicine. J Altern Complement Med 8: 703-717.

24. Trivedi MK, Branton A, Trivedi D, Nayak G, Sethi KK, et al. (2016) Isotopic abundance ratio analysis of biofield energy treated indole using gas chromatography-mass spectrometry. Science Journal of Chemistry 4: 41-48.

25. Trivedi MK, Branton A, Trivedi D, Nayak G, Panda P, et al. (2016) Evaluation of the isotopic abundance ratio in biofield energy treated resorcinol using gas chromatography-mass spectrometry technique. Pharm Anal Acta 7: 481.

26. Trivedi MK, Tallapragada RM, Branton A, Trivedi D, Nayak G, et al. (2015) evaluation of atomic, physical, and thermal properties of bismuth oxide powder: An impact of biofield energy treatment. American Journal of Nano Research and Applications 3: 94-98.

27. Trivedi MK, Tallapragada RM, Branton A, Trivedi D, Nayak G, et al. (2015) Evaluation of physical and structural properties of biofield energy treated barium calcium tungsten oxide. Advances in Materials 6: 95-100.

28. Trivedi MK, Nayak G, Patil S, Tallapragada RM, Latiyal O (2015) Studies of the atomic and crystalline characteristics of ceramic oxide nano powders after bio field treatment. Ind Eng Manage 4: 161-166.

29. Trivedi MK, Nayak G, Patil S, Tallapragada RM, Mishra R (2015) Influence of biofield treatment on physicochemical properties of hydroxyethyl cellulose and hydroxypropyl cellulose. J Mol Pharm Org Process Res 3: 126-133.

30. Trivedi MK, Branton A, Trivedi D, Gangwar M, Jana S (2015) Antimicrobial susceptibility, biochemical characterization and molecular typing of biofield treated *Klebsiella pneumoniae*. J Health Med Inform 6: 206.

31. Trivedi MK, Branton A, Trivedi D, Nayak G, Gangwar M, et al. (2015) Antibiogram, biochemical reactions, and genotypic pattern of biofield treated *Pseudomonas aeruginosa*. J Trop Dis 4:181.

32. Trivedi MK, Branton A, Trivedi D, Nayak G, Bairwa K, et al. (2015) Effect of biofield treatment on physical, thermal, and spectral properties of SFRE 199-1 mammalian cell culture medium. Advances in Biochemistry 3: 77-85.

33. Trivedi MK, Branton A, Trivedi D, Nayak G, Bairwa K, et al. (2015) Physical, thermal, and spectroscopic characterization of biofield energy treated Murashige and Skoog plant cell culture media. Cell Biology 3: 50-57.

34. Trivedi MK, Branton A, Trivedi D, Nayak G, Gangwar M, et al. (2015) Agronomic characteristics, growth analysis, and yield response of biofield treated mustard, cowpea, horse gram, and groundnuts. International Journal of Genetics and Genomics. 3: 74-80.

35. Trivedi MK, Branton A, Trivedi D, Nayak G, Mondal SC, et al. (2015) Evaluation of plant growth, yield and yield attributes of biofield energy treated mustard (*Brassica juncea*) and chick pea (*Cicer arietinum*) Seeds. Agriculture, Forestry and Fisheries. 4: 291-295.

36. Trivedi MK, Mohan R, Branton A, Trivedi D, Nayak G, et al. (2015) Evaluation of biofield energy treatment on physical and thermal characteristics of selenium powder. Journal of Food and Nutrition Sciences 3: 223-228.

37. Trivedi MK, Tallapragada RM, Branton A, Trivedi D, Nayak G, et al. (2015) Physicochemical characterization of biofield energy treated calcium carbonate powder. American Journal of Health Research 3: 368-375.

38. (1997) Desktop X-ray Diffractometer “MiniFlex+” The Rigaku Journal 14: 29-36.

39. Zhang T, Paluch K, Scalabrino G, Frankish N, Healy AM, et al. (2015) Molecular structure studies of (1S,2S)-2-benzyl-2,3-dihydro-2-(1Hinden-2-yl)-1H-inden-1-ol. J Mol Struct 1083: 286-299.

40. Langford JI, Wilson AJC (1978) Scherrer after sixty years: A survey and some new results in the determination of crystallite size. J Appl Cryst 11: 102-113.

41. Trivedi MK, Sethi KK, Panda P, Jana S (2017) A comprehensive physicochemical, thermal, and spectroscopic characterization of zinc (II) chloride using X-ray diffraction, particle size distribution, differential scanning calorimetry, thermogravimetric analysis/differential thermogravimetric analysis, ultraviolet-visible, and Fourier transform-infrared spectroscopy. International Journal of Pharmaceutical Investigation 7: 33-40.

42. Trivedi MK, Sethi KK, Panda P, Jana S (2017) Physicochemical, thermal and spectroscopic characterization of sodium selenate using XRD, PSD, DSC, TGA/DTG, UV-vis, and FT-IR. Marmara Pharmaceutical Journal 2: 311-318.

43. Raza K, Kumar P, Ratan S, Malik R, Arora S (2014) Polymorphism: The phenomenon affecting the performance of drugs. SOJ Pharm Pharm Sci 1: 10.

44. Brittain HG (2009) Polymorphism in pharmaceutical solids in Drugs and Pharmaceutical Sciences. (2nd Edition), Informa Healthcare, USA.

45. Censi R, Martino PD (2015) Polymorph impact on the bioavailability and stability of poorly soluble drugs. Molecules 20: 18759-18776.

46. Blagden N, de Matas M, Gavan PT, York P (2007) Crystal engineering of active pharmaceutical ingredients to improve solubility and dissolution rates. Adv Drug Deliv Rev 59: 617-630.

47. Chereson R (2009) Bioavailability, bioequivalence, and drug selection. In: Makoid CM, Vuchetich PJ, Banakar UV (eds) Basic pharmacokinetics (1st edition) Pharmaceutical Press, London.

48. Khadka P, Ro J, Kim H, Kim I, Kim JT, et al. (2014) Pharmaceutical particle technologies: An approach to improve drug solubility, dissolution and bioavailability. Asian J Pharm Sci 9: 304-316.

49. Lv X, Zhao M, Wang Y, Hu X, Wu J, et al. (2016) Loading cisplatin onto 6-mercaptopurine covalently modified MSNS: A nanomedicine strategy to improve the outcome of cisplatin therapy. Dovepress 10: 3933-3946.

50. Zhao Z, Xie M, Li Y, Chen A, Li G, et al. (2015) Formation of curcumin nanoparticles *via* solution-enhanced dispersion by supercritical CO_2. Int J Nanomedicine 10: 3171-3181.